

## MIT Open Access Articles

*Drainage canals in Southeast Asian  
peatlands increase carbon emissions*

The MIT Faculty has made this article openly available. **Please share** how this access benefits you. Your story matters.

**Citation:** Dadap, N. C., Hoyt, A. M., Cobb, A. R., Oner, D., Kozinski, M., Fua, P. V., et al. (2021). Drainage canals in Southeast Asian peatlands increase carbon emissions. *AGU Advances*, 2, e2020AV000321

**As Published:** 10.1029/2020AV000321

**Publisher:** American Geophysical Union (AGU)

**Persistent URL:** <https://hdl.handle.net/1721.1/132970>

**Version:** Final published version: final published article, as it appeared in a journal, conference proceedings, or other formally published context

**Terms of use:** Creative Commons Attribution 4.0 International license





## RESEARCH ARTICLE

10.1029/2020AV000321

## Drainage Canals in Southeast Asian Peatlands Increase Carbon Emissions

## Key Points:

- We created the first map of drainage canals across Southeast Asian peatlands and find that they are present across 65% of the region
- There is substantial variation in drainage density within land use types, indicating that land use is an incomplete proxy for drainage
- Peat subsidence rates and associated carbon emissions are higher in areas with progressively more drainage canals

## Supporting Information:

- Supporting Information S1
- Original Version of Manuscript
- Peer Review History
- First Revision of Manuscript [Accepted]
- Author Response to Peer Review Comments

## Correspondence to:

N. C. Dadap,  
[ndadap@stanford.edu](mailto:ndadap@stanford.edu)

## Citation:

Dadap, N. C., Hoyt, A. M., Cobb, A. R., Oner, D., Kozinski, M., Fua, P. V., et al. (2021). Drainage canals in Southeast Asian peatlands increase carbon emissions. *AGU Advances*, 2, e2020AV000321. <https://doi.org/10.1029/2020AV000321>

Received 16 OCT 2020  
 Accepted 7 FEB 2021

**Peer Review** The peer review history for this article is available as a PDF in the Supporting Information.

## Author Contributions:

**Conceptualization:** Nathan C. Dadap, Alison M. Hoyt, Alexander R. Cobb, Charles F. Harvey, Alexandra G. Konings

Nathan C. Dadap<sup>1</sup> , Alison M. Hoyt<sup>2,3</sup> , Alexander R. Cobb<sup>4</sup> , Doruk Oner<sup>5</sup> , Mateusz Kozinski<sup>5</sup> , Pascal V. Fua<sup>5</sup> , Krishna Rao<sup>1</sup> , Charles F. Harvey<sup>6</sup> , and Alexandra G. Konings<sup>1</sup>

<sup>1</sup>Department of Earth System Science, Stanford University, Stanford, CA, USA, <sup>2</sup>Max Planck Institute for Biogeochemistry, Jena, Germany, <sup>3</sup>Lawrence Berkeley National Laboratory, Berkeley, CA, USA, <sup>4</sup>Center for Environmental Sensing and Modeling, Singapore-MIT Alliance for Research and Technology, Singapore, Singapore, <sup>5</sup>École Polytechnique Fédérale de Lausanne, Lausanne, Switzerland, <sup>6</sup>Department of Civil and Environmental Engineering, Massachusetts Institute of Technology, Cambridge, MA, USA

**Abstract** Drainage canals associated with logging and agriculture dry out organic soils in tropical peatlands, thereby threatening the viability of long-term carbon stores due to increased emissions from decomposition, fire, and fluvial transport. In Southeast Asian peatlands, which have experienced decades of land use change, the exact extent and spatial distribution of drainage canals are unknown. This has prevented regional-scale investigation of the relationships between drainage, land use, and carbon emissions. Here, we create the first regional map of drainage canals using high resolution satellite imagery and a convolutional neural network. We find that drainage is widespread—occurring in at least 65% of peatlands and across all land use types. Although previous estimates of peatland carbon emissions have relied on land use as a proxy for drainage, our maps show substantial variation in drainage density within land use types. Subsidence rates are 3.2 times larger in intensively drained areas than in non-drained areas, highlighting the central role of drainage in mediating peat subsidence. Accounting for drainage canals was found to improve a subsidence prediction model by 30%, suggesting that canals contain information about subsidence not captured by land use alone. Thus, our data set can be used to improve subsidence and associated carbon emissions predictions in peatlands, and to target areas for hydrologic restoration.

**Plain Language Summary** Tropical peatlands are swamp-like environments in which naturally wet conditions slow the decomposition of plant carbon that would otherwise be released to the atmosphere. However, over the past few decades, humans have built drainage canals in Southeast Asian peatlands, due to economic pressure for logging and agriculture. These canals are a major threat to peatlands because they dry out peat soils, in turn speeding up decomposition and making soils susceptible to wildfire. Both of these mechanisms release massive amounts of carbon dioxide to the atmosphere, thereby accelerating climate change. Despite these risks, until now the extent of drainage in peatlands was unknown due to a lack of drainage canal maps. Here, we create the first regional map of drainage canals by training a computer algorithm to identify canals within high-resolution satellite images. We find that drainage is widespread—occurring in at least 65% of Southeast Asian peatlands. Furthermore, we find that more drainage canals are related to progressively larger subsidence rates—deformations in the ground surface partly caused by carbon dioxide emissions to the atmosphere. These findings suggest that it is important to know where and how much drainage is occurring to accurately predict subsidence and target areas for restoration.

## 1. Introduction

Hydrology governs carbon storage dynamics in tropical peatlands (Cobb et al., 2017; Dommain et al., 2010; Hirano et al., 2009). In these wetland environments, persistent flooding and anoxic conditions suppress decomposition rates, allowing organic material to accumulate over time in deep peat deposits. This process, compounded over millennia, has made Southeast Asian (SEA) peatlands one of the world's largest terrestrial pools of organic carbon: an estimated 67 Gt of carbon are stored in peatlands in Indonesia, Malaysia, and Brunei (Page et al., 2011; Warren et al., 2017). In recent decades, this carbon sink has been

© 2021. The Authors.

This is an open access article under the terms of the [Creative Commons Attribution License](https://creativecommons.org/licenses/by/4.0/), which permits use, distribution and reproduction in any medium, provided the original work is properly cited.

**Methodology:** Nathan C. Dadap, Doruk Oner, Mateusz Kozinski, Pascal V. Fua

**Validation:** Nathan C. Dadap, Doruk Oner, Krishna Rao

**Writing – original draft:** Nathan C. Dadap, Alexandra G. Konings

**Writing – review & editing:** Nathan C. Dadap, Alison M. Hoyt, Alexander R. Cobb, Doruk Oner, Mateusz Kozinski, Pascal V. Fua, Krishna Rao, Charles F. Harvey, Alexandra G. Konings

threatened by human disturbance (Leifeld & Menichetti, 2018). Widespread deforestation and conversion of peat swamp forests for agricultural use since the 1980s have left only ~6% of primary forests intact (Miettinen et al., 2016). Just as importantly, drainage canals constructed for transporting forestry products and improving agricultural yields (Bader et al., 2018) directly impact local hydrology by lowering water tables (Hooijer et al., 2010; Lim et al., 2012).

Hydrologic changes in peatlands have the potential to destabilize long-term peat carbon stocks, resulting in considerable carbon emissions. In situ studies measuring soil CO<sub>2</sub> flux found that decomposition rates are closely linked to water table depth (e.g., Hirano et al., 2009; Hoyt et al., 2019; Jauhiainen et al., 2005). As soils dry out, aerobic respiration increases, in turn causing higher CO<sub>2</sub> fluxes that result in peatland subsidence (Couwenberg et al., 2010; Hooijer et al., 2012; Jauhiainen et al., 2012). These potential emissions are substantial, as a recent study estimated that tropical peatland emissions due to drainage may comprise over one third of the greenhouse gas budget for keeping global temperature rise below 2°C (Leifeld et al., 2019). Peat fires, which also release massive amounts of carbon dioxide (Page et al., 2002) and cause regional haze events with widespread human health effects (Kopplitz et al., 2016), have grown in recent decades, indicating that drainage is drying out peatlands on a large scale (Dadap et al., 2019; Field et al., 2009). Furthermore, drainage canals increase fluvial export of dissolved organic carbon (Gandois et al., 2020; Moore et al., 2013).

Drainage of peatlands drives each of the regions' major carbon emissions mechanisms. However, the extent, distribution, and spatial patterns of drainage canals are unknown. As a result, all recent studies estimating regional carbon emissions have instead relied on emissions factors based on land use and land cover type (e.g., Carlson et al., 2013; Hiraishi et al., 2014; Leifeld & Menichetti, 2018; Miettinen et al., 2017; Murdiyarso et al., 2010). Such estimates implicitly rely on the assumption that drainage characteristics are linked to land use type. However, land use classifications neglect differences in drainage practices (e.g., prevalence of drainage canals, canal and water table depth, canal maintenance, etc.) that may vary widely within a given land use class. Consequently, the use of land use-based emissions factors to estimate peatland subsidence and associated carbon emissions at larger scales may introduce significant inaccuracies.

Here, we address these gaps by answering three central questions regarding hydrologic disturbance in SEA peatlands: 1) How widespread are drainage canals? 2) How does drainage differ between land use classes? and 3) Does drainage predict subsidence associated with peat oxidation at large scales? To answer these questions, we created the first region-wide, high-resolution (5 m) map of drainage canals in SEA peatlands, then compared drainage canal density to land use and subsidence data. We found that drainage is widespread and that drainage varies considerably within land use types. Peat subsidence is higher in areas with progressively higher drainage canal density throughout the region. Furthermore, accounting for drainage canals was found to substantially improve a subsidence prediction model, suggesting that canals contain information about subsidence not captured by land use alone.

## 2. Data and Methods

### 2.1. Development of Drainage Canal and Drainage Density Maps

We mapped drainage canals across SEA peatlands, an area that encompasses 157,000 km<sup>2</sup> on the islands of Sumatra and Borneo, and on Peninsular Malaysia (~6°S-6°N and 95°E-120°E). This region is estimated to contain ~53% of all soil carbon stored in tropical peatlands (Dargie et al., 2017; Page et al., 2011; Warren et al., 2017). In addition to 5 m resolution maps of drainage canals, we also created a second map depicting drainage density at 1 km resolution, defined here and throughout the manuscript as the length of drainage canals per unit area (in units of km/km<sup>2</sup>). We chose 1 km resolution for mapping drainage density because it is sufficiently coarse to reduce noise in the 5 m canal map but fine enough to capture land use features in this region.

#### 2.1.1. Satellite Imagery

To create the drainage canal map, we trained a model to identify canals within high-resolution satellite images from 2017 produced by Planet Labs, Inc. (“Planet”) (Planet Team, 2017). This data set has wall-to-wall coverage throughout the study area at high, 5 m resolution. Here, we used the “global\_quarterly\_2017q3\_mosaic Basemap” product, which is a global mosaic of RGB images taken by the PlanetScope constellation

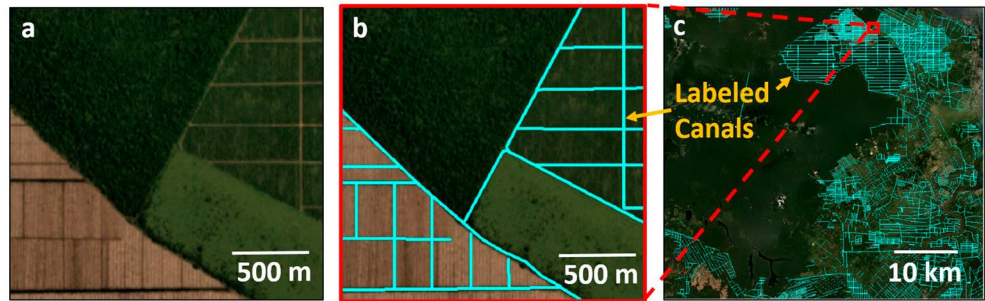


**Figure 1.** Training data for canal classification. (a) Example of 5 m resolution Planet Basemaps imagery used for identifying drainage canals. (b) Hand-labeled canals in turquoise overlay example image. (c) Full training data set in Riau Province, Sumatra, Indonesia. Training area ( $\sim 2,500 \text{ km}^2$ ) spans all land use types and a wide range of canal densities.

of CubeSat sensors between July and September 2017. This data set has two salient features that make it well-suited for the canal classification task. First, it has high—5 m—resolution that is necessary (Wedeux et al., 2020) for identifying narrow drainage canals that can be just meters in width (Evans et al., 2019; Jauhainen & Silvennoinen, 2012). Second, this data set exhibits very low ( $\sim 0.2\%$ ) cloud cover because Planet’s mosaicking algorithm layers images according to a ranking of image quality based on cloud cover and sharpness. The July–September time period was selected because it coincides with the SEA dry season (Aldrian & Dwi Susanto, 2003), further reducing cloud contamination in the data set. The Basemap data was used without further correction or alteration.

### 2.1.2. Training, Validation, and Test Data

To our knowledge, there are no publically available drainage canal maps in the study area that could be used for model development with complete and correct data, as well as accurate georeferencing to within a few meters. Even at the sub-regional scale, such maps are not available. Some hand-labeled canals are delineated in Open Street Maps, but these data appear to be intermittent and of unknown origin and accuracy, likely due to the fact that labeled data on that platform are open source and contributor-driven. Thus, it is difficult to gauge the accuracy, completeness, and possible biases in the data, and cannot be easily used for scientific research on drainage extent. Instead, we generated training, validation, and test data by manually labeling the Planet Basemap satellite images (Figure 1). This process was performed in Google Earth Engine (Gorelick et al., 2017) by hand-tracing canals with line vectors, then extruding them to create a raster image of canal labels. We also labeled roads as canals because we assume that roads are accompanied by drainage ditches and/or may inadvertently result in peatland drainage (Miettinen et al., 2012). While violations of this assumption could add uncertainty to our drainage density estimates, we believe such instances are rare; peat has extremely low load bearing capacity and does not have natural drainage, suggesting that ditches are generally necessary for road use and maintenance akin to other tropical, high-rainfall environments (Barry et al., 1992; Lim et al., 2012). We filter out “urban” peatlands (as classified by Miettinen et al. [2016]) from our analyses where the road-canal relationship may differ due to increased density of road and concrete ground cover. In total, the labeled imagery spans  $\sim 2,500 \text{ km}^2$  across multiple land use types in the Bengkalis and Siak Regencies in Riau Province, Sumatra, Indonesia.

We also labeled images to generate validation and test data sets for assessing out-of-sample accuracy (Figures S1 and S2 in the supporting information). Test data differs from the validation data in that it was labeled by an independent labeler, allowing for an assessment of potential systematic bias from human labeling error. The validation area was comprised of  $\sim 100 \text{ km}^2$  or 4% of the labeled data in Riau, and were selected to span multiple land use types and drainage densities. Test data locations were selected for four areas spread across the study area, chosen via stratified random sampling (Figure S2).

### 2.1.3. Classification Methodology

A convolutional neural network (CNN) was used to identify drainage canals within the satellite imagery. Originally developed in the context of handwriting recognition (LeCun et al., 1998), CNNs have seen an

increase in usage since 2012, when they were shown to achieve superior performance in image classification tasks (Krizhevsky et al., 2017). Pixel by pixel classification schemes fail at identifying drainage canals in images because canals exhibit variable radiative spectral signatures; canals can be covered by open water, soil, or vegetation when covered by canopy or overgrown brush. Thus, the ability of CNNs to consider the context around a pixel to identify linear shapes is of paramount importance for canal identification. We further used a state of the art canal-segmentation algorithm that was originally designed to identify roads from satellite imagery (Oner et al., 2020) because canals, like roads, are narrow linear features of varying width. This algorithm uses a recurrent CNN with U-Net architecture (Ronneberger et al., 2015), and, unlike other CNN algorithms, incorporates in its objective function loss terms that promote global connectivity. As a result, it outperforms other state of the art methods. The algorithm was written in PyTorch and partially implemented in C++ for increased speed. Training of the network took 5–6 days and prediction took ~5–10 s per tile for 1664 image tiles in this region on a Tesla V100-SXM2-32GB GPU processor. The code is available at <https://github.com/doruk-oner/TOPO-Windowed-Loss> and further description of the specific algorithm can be found in Oner et al. (2020).

#### 2.1.4. Model Assessment

We assessed canal map accuracy using the quality metric, which is defined as the number of true positives divided by the sum of true positives, false positives, and false negatives. This metric is commonly used in road mapping classification, and is more appropriate than the accuracy metric (defined as the number of true positives divided by the sum of true positives, true negatives, false positives, and false negatives) due to a high number of true non-canal pixels (Wiedemann et al., 1998). As noted in Oner et al. (2020), the definition of a true positive was relaxed to allow for positive matches within a distance of 5 pixels, to avoid penalizing the results for minor spatial mismatches in canal location. We also evaluated the accuracy of drainage density measurements by calculating the squared Pearson correlation coefficient ( $r^2$ ), root-mean-squared-error (RMSE), and bias between retrieved drainage density data to validation and test data sets at 1 km resolution. While classification results would ideally be compared to an independent “true” data set that is based on ground-truthed data of canal locations, such a data set does not exist in this region. As such, manually labeled satellite images are currently the best method for generating training and validation data for canal mapping.

## 2.2. Land Use Analyses

To better understand the relationship between drainage and land use, we compared drainage density to land use data obtained from maps by Miettinen et al. (2016), which are based on hand-delineation of 2015 Landsat images. Our analyses were conducted at 1 km resolution to match the selected resolution of our drainage density map. We filtered out pixels where the most common land use type did not constitute an absolute majority of the pixel. In accordance with the changes in land use classes applied by Miettinen et al. (2017), the “Seasonal water,” “Ferns/low shrub,” and “Clearance” categories were combined under the “Open undeveloped” designation, to better reflect land use classes used in IPCC emissions factors. These three land use classes are similarly characterized by little to no vegetation cover (<2 m high) and lack of agricultural development. Drainage density categories were defined by binning drainage density values into four classes, as shown in Equation 1. Examples of canal networks based on these drainage density categories are shown in Figures 4 and S3.

$$\text{Drainage density category} = \begin{cases} \text{None} & \text{Drainage density} = 0 \text{ km} / \text{km}^2 \\ \text{Low} & 0 \text{ km} / \text{km}^2 < \text{Drainage density} \leq 2.5 \text{ km} / \text{km}^2 \\ \text{Moderate} & 2.5 \text{ km} / \text{km}^2 < \text{Drainage density} \leq 5 \text{ km} / \text{km}^2 \\ \text{High} & 5 \text{ km} / \text{km}^2 < \text{Drainage density} \end{cases} \quad (1)$$

## 2.3. Subsidence Analyses

We analyzed the relationship between drainage and subsidence by comparing to data from Hoyt et al. (2020), who measured subsidence across eight 100 × 100 km frames in the study area. These data were measured using interferometric synthetic aperture radar (InSAR) data from Japan Aerospace Exploration Agency's



Advanced Land Observing Satellite (ALOS-1), and are the only subsidence measurements in SEA peatlands available over a large area. InSAR-based subsidence measurement involves measuring phase changes in the reflected radar beam between subsequent passes of an observing satellite, allowing for millimeter-scale sensitivity to changes in elevation. We then estimated carbon fluxes associated with the subsidence data using the approach outlined by Hoyt et al. (2020), as described further in Text S1 of the supporting information (Couwenberg & Hooijer, 2013; Leifeld et al., 2011; van den Akker et al., 2008; Van den Wyngaert, 2008). These estimates are not presented for use as emissions factors, but rather to provide a rough estimate of emissions associated with subsidence due to drainage; these estimates are uncertain due in part to the fact that subsidence rates are determined not only by oxidation, but also compaction, shrinkage, and consolidation of peat at lower depths (Hooijer et al., 2012). Note that these data represent the period 2007–2011, 6–10 years before the drainage estimates.

We plotted probability distributions of subsidence as grouped by drainage density using kernel density estimation. The median subsidence and standard error were then calculated for each distribution. An independent sample *t*-test without assumption of equal variance was applied to each pair of distributions; *p* values  $\ll 0.01$  for all combinations imply that the difference in mean subsidence between all drainage groups is statistically significant. Due to the  $\sim 8$  year temporal mismatch between the subsidence and drainage density data sets, we present results only for areas where land use change did not occur between 2007 and 2015; land use type for a given year was defined as the most common land use type in a given  $1 \times 1$  km pixel that constituted an absolute majority (50%) of the pixel. Of the 11,408 pixels where subsidence measurements were available, 89% (or  $n = 10,182$ ) remained the same dominant land use in 2015 as in 2007. However, inclusion of the remaining pixels where land use change did occur did not significantly change the model results.

We further assessed the value of drainage metrics in predicting subsidence by creating a random forest model for subsidence, then evaluating the increase in model explanatory skill (as calculated by the coefficient of determination  $R^2$ ) when including drainage metrics. The non-drainage predictor features used were land use type and distance to peat edge (Text S2)—two features that were previously used to predict subsidence at regional scales (Hoyt et al., 2020)—and VIIRS 375 m active fire count aggregated to 1 km (Schroeder et al., 2014), which was assumed to contain information regarding the hydrologic state of a given area because of the sensitivity of burned area to soil moisture and burn depth to water table depth (Dadap et al., 2019; Usup et al., 2004). The drainage metrics used were drainage density (with continuous values, rather than discretized by categories) and average distance to canals. Both were calculated at 1 km resolution from the 5 m resolution canal map. Although drainage density and distance to canals have an inverse relationship (Figure S4), it is not exactly one-to-one, depending on the details of the canal geometry in a given location. Furthermore, distance to canals is a potentially more informative predictor of subsidence (relative to drainage density alone), since it is expected to more closely match the effect of canals on nearby water table depths than drainage density alone (Sinclair et al., 2020). Thus, we chose to include both drainage metrics in the model. Additional details on the development of the random forest subsidence model are provided in Text S2 of the supporting information.

### 3. Results

#### 3.1. Canal Classification Accuracy

Our canal classification map exhibits high accuracy in the validation and test areas. Visual inspection of the 5 m resolution canal map show that the classification captures the overall spatial patterns of drainage canals (Figures S1 and S2). The data set displays a quality score of 0.85 in the validation area, a value that compares favorably to recent road mapping efforts (Oner et al., 2020). Because traditional binary classification metrics are highly imbalanced for canal maps (since most pixels are non-canals), we also assessed model performance on drainage density data aggregated to  $1 \times 1$  km resolution. To make this comparison, we created a map of drainage density (Methods, Figure 3a). Drainage density results in the validation area displayed high correlation with hand-labeled drainage density data ( $r^2 = 0.89$ , RMSE =  $0.77 \text{ km/km}^2$ ) and were slightly conservative (underestimation of drainage density with bias =  $-0.47 \text{ km/km}^2$  vs. mean  $3.08 \text{ km/km}^2$ ; Figure 2a). A comparison to a separate test data set was also performed; the test data differs from the validation data in that it was labeled by an independent labeler, allowing for an assessment of

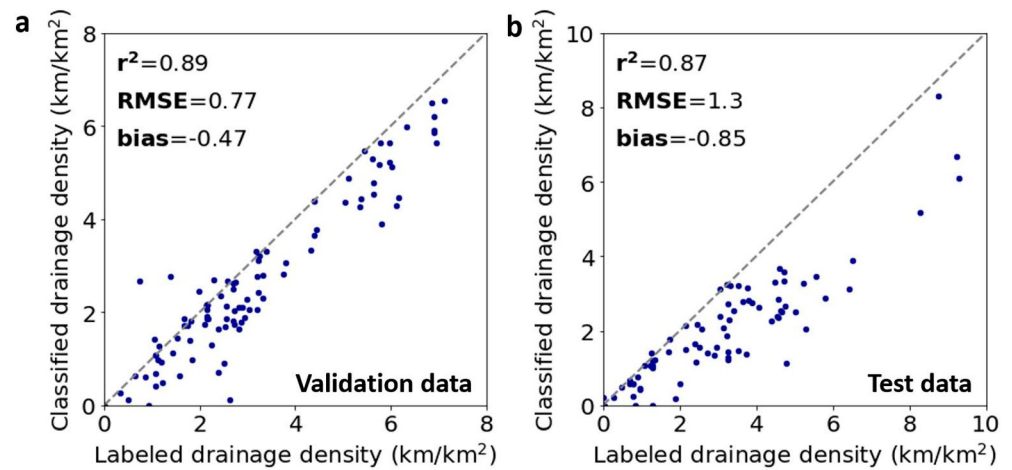


**Figure 2.** Canal classification performance. Scatterplots showing drainage density of classified canals versus drainage density of labeled canals in (a) validation and (b) test areas.

potential systematic bias from human labeling error. Similar performance between the validation and test results ( $r^2 = 0.83$ ,  $RMSE = 1.3 \text{ km/km}^2$ ,  $bias = -0.85 \text{ km/km}^2$ ; Figure 2b) suggest that there is no significant bias in the results due to labeling error.

### 3.2. Extensive Drainage in SEA Peatlands

Our drainage density map (Figure 3a) reveals that drainage is widespread: 65% of  $1 \times 1 \text{ km}$  pixels (spanning  $93,000 \text{ km}^2$ ) in SEA peatlands were found to contain drainage canals. Given the 5 m resolution of the input images, these results pertain only to canals  $\geq 5 \text{ m}$  width. The omission of narrow canals, in addition to the fact that the model exhibits negative bias, suggest that the true percentage of drained peatlands is likely even higher than the 65% estimate determined here.

There are notable spatial patterns of drainage density within the drainage canal maps (Figures 3b and 3c). For example, in northern Borneo, there is an abrupt shift in drainage density across the border between Malaysia and Brunei, corresponding to differences between plantations and conservation areas in each of the two countries. Similarly, areas in Central Kalimantan within the ex-Mega Rice Project area (much of which underwent widespread and intensive drainage in the 1990s [Houterman & Ritzema, 2009]) still exhibit higher drainage densities than in the adjacent and relatively protected Sebangau National Park, which has little drainage. Accordingly, this map of drainage density (Figure 3a) and the 5 m resolution canal map (examples shown in Figures 3b and 3c) depict varying degrees of peatland hydrologic disturbance.

For subsequent analyses, we grouped the data into drainage density categories to reduce the sensitivity of our results to classification error. These encompass categories of None (no canals detected), Low ( $0\text{--}2.5 \text{ km/km}^2$ ), Moderate ( $2.5\text{--}5 \text{ km/km}^2$ ), and High ( $>5 \text{ km/km}^2$ ) drainage density. To illustrate these categories, examples of the spatial pattern of canals underlying each category are shown in Figures 4 and S3. Areas with High or Moderate drainage density are generally indicative of dense, systematic drainage networks and account for 37% ( $\sim 36,000 \text{ km}^2$ ) of all drained peatlands.

### 3.3. Drainage Density Varies Within Land Use Types

Across all of the major land use categories considered, except pristine forests, there is substantial variation in drainage density. For example, in industrial plantations, Moderate drainage density occurs in 51% of plantations and Low drainage density in 34% (Figure 5a). Similarly, areas classified as smallholder plantations, open undeveloped, and degraded forest areas also exhibit considerable variation in drainage density, with each of these land use types containing at least two drainage density categories that span 15% of its area or more (Table S1). Overall, the variation in drainage density within each land use type (Figure 5a)

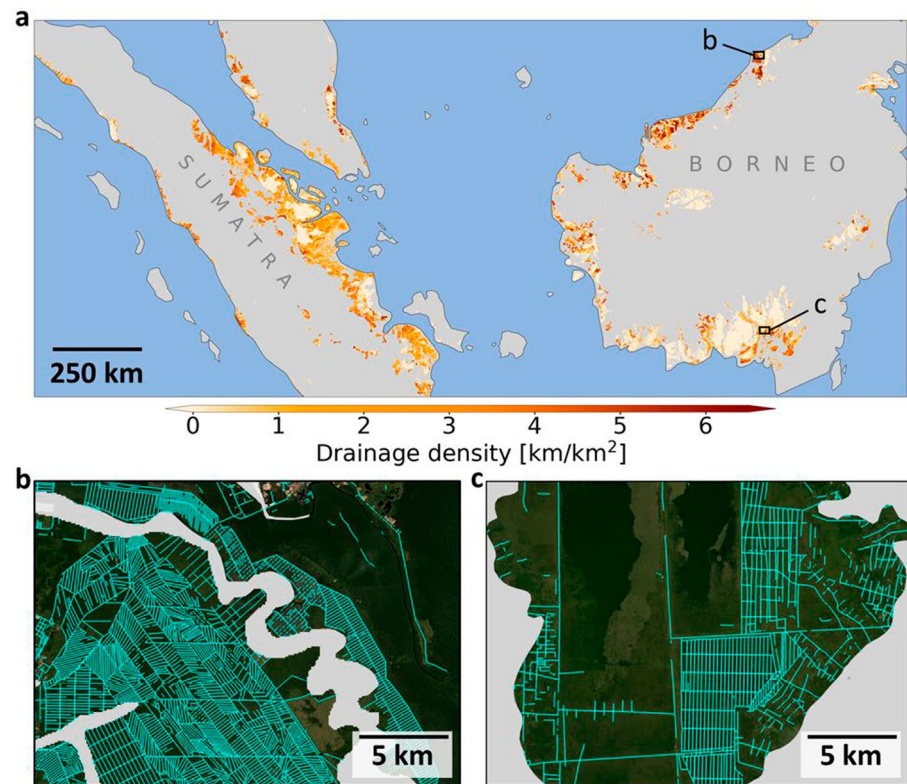


**Figure 3.** Canal classification results. (a) Map of drainage density [canal length per peat area, km/km<sup>2</sup>] across SEA peatlands at 1 km resolution as retrieved from 2017 satellite imagery. Non-peatland areas are shown in gray. Black callouts outline example areas showing 5 m resolution canal maps in (b) Sarawak, Malaysia/Belait, Brunei, and (c) Block B of the former Mega Rice Project area in Central Kalimantan, Indonesia.

indicates that land use classifications alone are insufficient to capture hydrologic impacts from drainage canals in SEA peatlands.

Drainage density is generally higher in industrial and smallholder plantations than in pristine forest, degraded forest, or open undeveloped areas. Plantations comprise 91% of areas that have High or Moderate drainage density, and industrial plantations make up 75% of those categories alone (Table S1). In contrast, areas with Low drainage density are more evenly distributed between smallholder plantations (42%), industrial plantations (24%), open undeveloped (18%), and degraded forest (13%) land use types (Figure 5b). Considerable peatland water management efforts and regulation have justifiably focused on drainage in industrial plantations (e.g., Lim et al., 2012; Republic of Indonesia, 2016). However, non-industrial plantation land uses comprise 57% of the total drained area.

### 3.4. Drainage Density Predicts Subsidence

In mapping peatland drainage across the region for the first time, we find that subsidence rates (and associated carbon emissions) are higher in areas with progressively higher drainage density. To assess the effect of drainage on subsidence, we compared drainage density to subsidence rates measured from 2007 to 2011 (Hoyt et al., 2020), and found that High drainage density areas have median subsidence rates that are 1.3X larger than in Moderate drainage density areas, 1.5X larger than in Low drainage density areas, and 3.2X larger than in areas with no drainage (Figure 6). This relationship holds even though drainage density data were measured 8 years after the subsidence measurements. The positive relationship between drainage density and subsidence, although not always evident, can sometimes be observed visually in maps depicting subsidence and canals, with several examples shown in Figure S5. Median subsidence values are significantly different between classes (for *t*-tests applied to distribution means, *p*-value << 0.01). However,



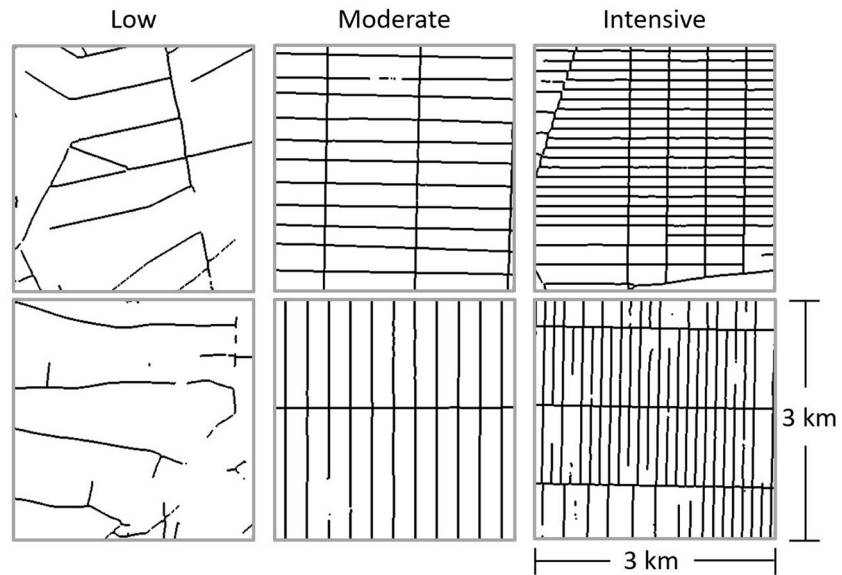


**Figure 4.** Examples of drainage density categories. Classified canals (black) are shown in  $3 \times 3$  km squares, sorted by drainage density categories in each column. Examples were selected from areas in Sarawak, Malaysia and West Kalimantan, Indonesia. Drainage density categories of Low, Moderate, and High drainage correspond to drainage densities of  $0\text{--}2.5$ ,  $2.5\text{--}5$ , and  $>5$   $\text{km}/\text{km}^2$ . Additional category examples are shown in Figure S3.

it should be noted that the relationship between drainage density and subsidence does not hold in the ex-Mega Rice Project area in Central Kalimantan, Indonesia (Figure S6, Table S3), likely due to the presence of deeper drainage canals and deeper overall water table depths in that area (see Section 4). Across all other areas, pixels with high drainage density have subsidence rates that are  $1.86 \pm 0.09$   $\text{cm}/\text{yr}$  greater than in areas with no drainage. These differences in subsidence rates potentially translate to significantly increased carbon fluxes, as  $\text{CO}_2$  emissions can be estimated based on characteristics of the peat lost during subsidence (see Section 2 and supporting information). Assuming a mean peat carbon content of 55% and dry bulk density of  $0.08$   $\text{g}/\text{cm}^3$  (Couwenberg & Hooijer, 2013), the subsidence rate in intensively drained areas corresponds to  $11.8 \pm 1.9$   $\text{tC}/\text{ha}/\text{yr}$  of emissions, a large flux relative to the  $3.6 \pm 0.6$   $\text{tC}/\text{ha}/\text{yr}$  emissions rate in areas where drainage canals were not detected.

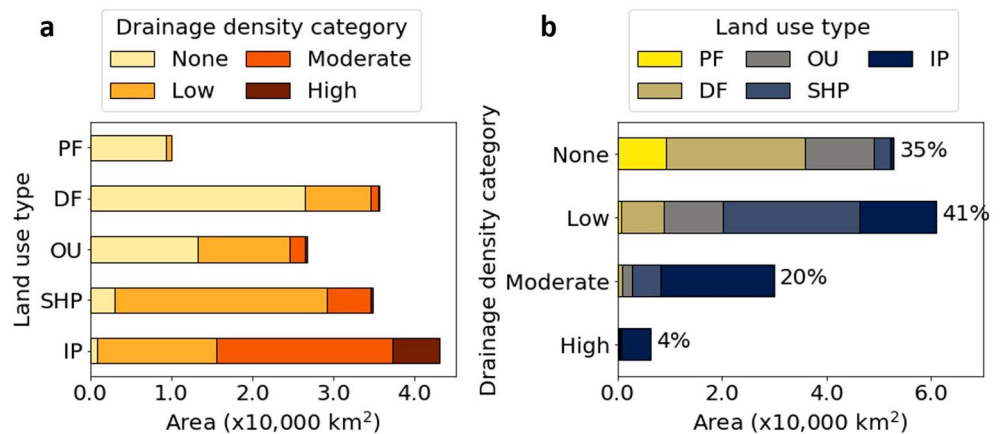


**Figure 5.** Distribution of drainage density in peatlands. (a) Land use types are subdivided by drainage density categories, defined as None (no detected canals), Low ( $0\text{--}2.5$   $\text{km}/\text{km}^2$ ), Moderate ( $2.5\text{--}5$   $\text{km}/\text{km}^2$ ), and High drainage ( $>5$   $\text{km}/\text{km}^2$ ). PF, pristine forest; DF, degraded forest; OU, open undeveloped; SHP, smallholder plantation; and IP, industrial plantation. (b) Drainage density categories are subdivided by land use type. The percent of total peatland area for a given drainage density is shown next to the bar.

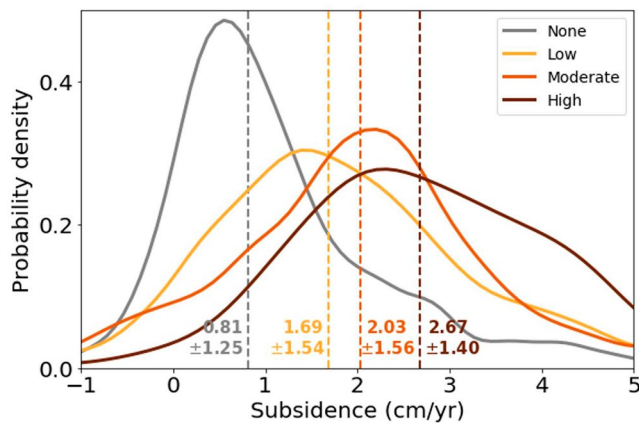


**Figure 6.** Relationship between subsidence and drainage density. Distribution of subsidence rates are shown for each drainage density category. Dashed vertical lines show medians for each distribution. Median  $\pm$  standard deviation is shown for each distribution next to median line. Positive subsidence denotes downward ground surface displacement and CO<sub>2</sub> release to the atmosphere. Subsidence was measured by Hoyt et al. (2020) using ALOS-1 PALSAR interferometric data from 2007 to 2011.

Accounting for drainage canals substantially improved our ability to predict subsidence rates, suggesting that drainage maps contain important hydrologic information not captured by land use alone. Here, we built a random forest model of subsidence (at 1 km resolution), and assessed model performance when including drainage metric inputs. Addition of drainage metrics to a model with land use, distance to peat edge, and active fire count as predictor variables increased the amount of explained variability in subsidence by 30% (from  $R^2 = 0.3-0.39$ ). Drainage metrics were the second most important category of information in the random forest model (Table S2), underscoring the importance of including canal-based drainage metrics in assessing peatland subsidence and associated carbon emissions.

## 4. Discussion

### 4.1. Implications of Widespread Drainage

We created the first region-wide map of drainage canals and found that a majority of SEA peatlands are drained (Figure 3a). This map makes it possible to disentangle drainage from land use. While most of the literature has focused on assessing impacts of drainage within the context of industrial plantations, we found that 57% of areas containing drainage canals (i.e., 57% of  $1 \times 1$  km tiles) are outside of industrial plantations, underscoring the importance of considering drainage impacts across all peatland land use types. Areas with Moderate and High drainage density are mainly comprised of industrial plantations (76%), and areas with Low drainage density are primarily smallholder plantations (43%). Land use has often been used to parameterize drainage in hydrologic models and for upscaling of carbon emissions estimates (e.g., Mezbahuddin et al., 2015; Miettinen et al., 2017; Taufik et al., 2020, and more). Indeed, land use was found to be the most important predictor of subsidence rates in our random forest models (Table S2). However, drainage density was found to vary within each land use type (Figure 5a). This suggests that while drainage may convey information about possible land use types, particularly for high drainage densities (Figure 5b), land use is an incomplete proxy for drainage in the region. Drainage metrics such as drainage density provide a means to compare hydrologic impacts at sub-regional scales even within homogenous land use types.

Drainage canals affect subsidence rates via a hydrologic link: drainage lowers water tables and dries out peat soils, which in turn increase peat oxidation (Carlson et al., 2015; Couwenberg & Hooijer, 2013; Couwenberg et al., 2010; Hooijer et al., 2010, 2012; Jauhiainen et al., 2012). While these mechanisms have previously only been demonstrated at local scales, our results confirm the importance of these relationships at regional scales, as subsidence is found to vary with drainage density across the region (Figure 6). This relationship holds despite a roughly 8 year difference between the subsidence data set (measured from 2007 to 2011) and the drainage density data set (2017) which likely adds noise to the relationship. Still, subsidence rates may be affected by land use change impacts apart from drainage. For example, non-drainage disturbances to peatlands include deforestation, use of fire to clear land, and conversion for agricultural use (Dohong et al., 2017). These disturbances, independent of drainage, may in turn cause secondary impacts to ecohydrological variables, such as water table depth (Hirano et al., 2009), soil physical properties such as bulk density, pore structure, and hydraulic conductivity (Kurnianto et al., 2018; Sinclair et al., 2020; Wells et al., 2016). They can also impact evapotranspiration due to shifts in photosynthetic rates and rooting depth (Hirano et al., 2015; Manoli et al., 2018). Such impacts may also partially explain why non-zero subsidence is evident in areas where drainage canals were not detected (Figure 6). Secondary impacts of land use interact with those attributable to drainage, and a full assessment of the effects on subsidence would likely require the use of a hydrologic model. While such an analysis is beyond the scope of this study, we verified the utility of drainage metrics independent of land use using an empirical, random forest model for subsidence. When accounting for drainage metrics in the model that already accounted for land use, we found an improvement in model performance of 40% (Table S2), suggesting that drainage provides significant

information about subsidence not captured in land use data alone. Thus, our results suggest that future estimates of peatland emissions associated with subsidence would benefit from inclusion of drainage metrics.

Drainage also increases peatland fire risk (van der Werf et al., 2008). In peatlands, organic soil is flammable if sufficiently dry, and only soil above the water table can catch fire (Usup et al., 2004). Accordingly, water tables lowered by drainage canals can increase the potential depth of peat fires and fire frequency (Konecny et al., 2016). Drainage impacts can extend beyond the areas adjacent to canals. For example, recent studies found that the presence of canals affected water table depths hundreds of meters away (Astiani et al., 2017; Evans et al., 2019) and forest biomass growth up to 1 km away (Wedeux et al., 2020). Accordingly, even isolated canals can have far-reaching hydrologic impacts via their impact on water tables in the surrounding area, underscoring the utility of their detection.

#### 4.2. Beyond Quantification of Drainage Density

The classification of narrow, linear features such as canals from satellite images requires high resolution imagery, and can only occur at the resolution of the input data. For example, recent attempts to identify logging canals in SEA found that canals were invisible using 30 m resolution Landsat images (Wedeux et al., 2020). Tree canopies can obscure narrow canals (Jaenicke et al., 2010), but the 5 m resolution data used here allows for increased visibility of narrower canals through some vegetation cover. Nevertheless, 5 m resolution is still too coarse to consistently capture drainage canals <5 m in width, which also contribute to peatland hydrologic disturbance. Thus, classification performance may be disproportionately worse in land use types with denser vegetation cover. Indeed, visual inspection of pixels with larger bias in the validation area suggest that lack of contrast between canals and surrounding vegetation may contribute to misclassification at this resolution, especially for thinner canals. Accordingly, we recommend that future efforts to map drainage canals use imagery at sub-1 m resolution where available. Airborne Lidar measurements can also be used for identifying narrow canals (Roelens et al., 2018), but may be costly to obtain. Information from additional sources (e.g., remote sensing images from different types of instruments) may also improve canal detection, and the deep learning model used here is flexible to allow for multiple input data sources. In particular, low frequency microwave observations that can penetrate vegetation could be promising for use in SEA peatlands (Dadap et al., 2019). However, the use of multiple sensors may also introduce georeferencing errors if there is any spatial mismatch between data sets. Ultimately, our validation results suggest that a single data source with 3 optical channels (red, green, and blue wavelength observations) was sufficient for classification of the >5 m canals identified here.

In contrast to the observed drainage-subsidence relationship (Figure 6) that exists throughout a majority of the region, the ex-Mega Rice Project area in Central Kalimantan (Figure S6, Table S3), exhibits high subsidence even in areas with low or no apparent drainage. This area also burns regularly (Vetrita & Cochrane, 2020), and fire events could directly lead to mass loss, compaction, and changes in microbial communities. Since both subsidence and fire are closely tied to hydrologic factors, a possible factor governing the anomalous behavior in this region may be the presence of deep drainage canals that lead to lower water table depths compared to the rest of SEA. In this area, canals are on average 2 m deep (significantly deeper than the average canal depth elsewhere in the region) and in some cases extend multiple meters down to the underlying clay substrata (Suryadiputra et al., 2005). Such deep canals coupled with a lack of flow control structures have resulted in canal water levels that are shifted multiple meters below the ground surface (Vernimmen et al., 2020b). Deep water levels within canals, in turn, will lower water table depths at further distances from the canals. In comparison, control structures such as weirs are now generally employed in other parts of the region (in part informed by the early failures of the ex-Mega Rice Project) aiming to maintain water table levels near the ground surface (Lim et al., 2012). Accordingly, tracking of canal water levels is needed to better understand the impact of drainage density and canal layout on water table depths away from canals. Lidar measurements, previously used in tropical peatlands for mapping carbon stocks (Vernimmen et al., 2020a) and for estimating carbon losses from burn scars (Ballhorn et al., 2009; Simpson et al., 2016) are especially promising for measuring canal water levels (Rahman et al., 2017; Vernimmen et al., 2020b). However, spaceborne lidar does not have sufficient density of sampling needed to cover all canals in the region, and airborne lidar measurements have only been made over a small fraction of the region. Thus, determining the width and depth of all the drainage canals mapped

here is not currently possible. Nevertheless, additional information about canal depth and density enabled by more widespread and frequent airborne lidar measurements would complement the drainage metrics introduced in this study.

### 4.3. Potential Applications of Canal Maps

In this study, we introduced a method for mapping drainage canals using satellite imagery and deep learning; our methodology is transferable to other geographic locations that are sensitive to drainage, such as temperate and boreal peatlands. Currently, drainage canals are less prevalent in other tropical peatlands such as those in the Congo and Amazon river basins, which have so far experienced less extensive land use change (Dargie et al., 2019; Lilleskov et al., 2019; van Lent et al., 2019). However, increasing economic pressure for timber extraction and oil palm, coupled with a dearth of protective regulations, indicate these basins are similarly vulnerable to the same path of peatland degradation as in SEA (Lilleskov et al., 2019). There has also been increased attention in restoring drained areas in European peatlands, where ditch characteristics combined with other predictors were found to be useful for evaluating peatland hydrological controls on greenhouse gas emissions (Bechtold et al., 2014). Thus, there is a clear need to track the global expansion of peatland drainage. The growing availability of publically available, high-resolution satellite imagery, combined with our classification method, open the door for monitoring drainage canal development in global peatlands across both space and time.

The drainage density maps produced here can also be used toward representing drainage in modeling studies, both at individual sites and across larger areas. Recent investigations to simulate water table depth have relied on assumptions of drainage based on land use type to parametrize subsurface flow and boundary conditions in hydrologic models (e.g., Mezbahuddin et al., 2015; Taufik et al., 2020). Other recent studies have modeled fire risk in peatlands considering a wide range of factors (e.g., Sloan et al., 2017; Sze & Lee, 2018), but similarly have had to rely on land use metrics and road data sets as a proxies for drainage, due to the lack of regional drainage density information. Our data set will facilitate more direct parametrization of drainage in both mechanistic and statistical modeling efforts.

In addition to drainage density, canal maps provide information about canal network shapes which, in conjunction with natural rivers, determine the carbon storage potential in peatlands by altering the shape of the water table (Cobb et al., 2017). The thickness of the vadose zone determines subsidence rates, so canal maps can provide information about which areas are likely to experience subsidence, as observed in Figure S5. Long-term peatland storage is also strongly governed by peat dome shape, which in turn is determined by boundary conditions. In drained systems, canal spacing limits the peat that can be preserved by waterlogging (Cobb et al., 2020), so canal maps are essential for determining the potential capacity for peat carbon storage. Accordingly, canal maps will be essential for determining not only carbon fluxes associated with subsidence in the present, but also long-term carbon storage potential for years to come.

Over the past decade, there has been increasing interest in the potential of peatland hydrological restoration to reduce greenhouse gas emissions (Leifeld et al., 2019; Morecroft et al., 2019; Tanneberger et al., 2020; Wilson et al., 2016). Drainage maps, combined with water management information regarding drainage control or rewetting, can be used to improve models of peatland water and carbon dynamics including more accurate emissions factors (Tiemeyer et al., 2020). Although questions remain about the potential for overall reductions in greenhouse gases, due to compensating methane emissions (Hemes et al., 2018), the long-term mitigation potential of rewetting via canal-blocking likely outweighs the increase in methane emissions (Günther et al., 2020). Indeed, there is evidence that drainage management and rewetting can result in decreased carbon emissions, increased biodiversity, and reduced fire (Cris et al., 2014; Hiraishi et al., 2014). Thus, an understanding of drainage conditions, including canal mapping, should be a crucial component for identifying areas of peatland degradation. When combined with other data sets in peatlands such as remotely sensed soil moisture (Dadap et al., 2019), our maps may help peatland managers prioritize areas for hydrologic restoration; canal maps allow for identification of areas where new or unexpectedly high drainage density is occurring. The results presented here further suggest that drainage canal maps could be used to more accurately represent peatland subsidence, associated carbon emissions, and hydrology, and therefore will serve as an important tool for protecting peatland ecosystems.



## Data Availability Statement

The drainage canal maps developed in this study are available for download at <https://doi.org/10.25740/yj761xk5815>. The code used to generate these maps are available at <https://github.com/doruk-oner/TOPO-Windowed-Loss>. Land use and subsidence data used in this study are available from Miettinen et al. (2016) and Hoyt et al. (2020), respectively.

## Acknowledgments

N. C. Dadap was supported by NASA Headquarters under the NASA Earth and Space Science Fellowship Program—Grant 80NSSC18K1341. This work is supported by NSF under Award EAR-1923478 to A. G. Konings and C. F. Harvey. This research was also supported by the National Research Foundation (NRF), Prime Minister's Office, Singapore under its Campus for Research Excellence and Technological Enterprise (CREATE) program and Grant No. NRF2016-ITCOO1-021. The Center for Environmental Sensing and Modeling (CENSAM) is an interdisciplinary research group (IRG) of the Singapore MIT Alliance for Research and Technology (SMART). D. Oner was supported by the Swiss National Science Foundation under Sinergia Grant 177237.

## References

- Aldrian, E., & Dwi Susanto, R. (2003). Identification of three dominant rainfall regions within Indonesia and their relationship to sea surface temperature. *International Journal of Climatology*, 23(12), 1435–1452. <https://doi.org/10.1002/joc.950>
- Astiani, D., Burhanuddin, B., Curran, L. M., Mujiman, M., & Salim, R. (2017). Effects of drainage ditches on water table level, soil conditions and tree growth of degraded peatland forests in West Kalimantan. *Indonesian Journal of Forestry Research*, 4(1), 15–25. <https://doi.org/10.20886/ijfr.2017.4.1.15-25>
- Bader, C., Müller, M., Schulin, R., & Leifeld, J. (2018). Peat decomposability in managed organic soils in relation to land use, organic matter composition and temperature. *Biogeosciences*, 15(3), 703–719. <https://doi.org/10.5194/bg-15-703-2018>
- Ballhorn, U., Siegert, F., Mason, M., & Limin, S. (2009). Derivation of burn scar depths and estimation of carbon emissions with LIDAR in Indonesian peatlands. *Proceedings of the National Academy of Sciences of the United States of America*, 106(50), 21213–21218. <https://doi.org/10.1073/pnas.0906457106>
- Barry, A., Brady, M., & Younger, J. (1992). Roads on peat in east Sumatra. *Geotechnical Engineering*, 23(1), 145–161.
- Bechtold, M., Tiemeyer, B., Laggner, A., Leppelt, T., Frahm, E., & Belting, S. (2014). Large-scale regionalization of water table depth in peatlands optimized for greenhouse gas emission upscaling. *Hydrology and Earth System Sciences*, 18(9), 3319–3339. <https://doi.org/10.5194/hess-18-3319-2014>
- Carlson, K. M., Curran, L. M., Asner, G. P., Pittman, A. M., Trigg, S. N., & Marion Adeney, J. (2013). Carbon emissions from forest conversion by Kalimantan oil palm plantations. *Nature Climate Change*, 3(3), 283–287. <https://doi.org/10.1038/nclimate1702>
- Carlson, K. M., Goodman, L. K., & May-Tobin, C. C. (2015). Modeling relationships between water table depth and peat soil carbon loss in Southeast Asian plantations. *Environmental Research Letters*, 10(7), 074006. <https://doi.org/10.1088/1748-9326/10/7/074006>
- Cobb, A. R., Dommain, R. R., Tan, F., Heng, N. H. E., & Harvey, C. F. (2020). Carbon storage capacity of tropical peatlands in natural and artificial drainage networks. *Environmental Research Letters*, 15, 23–25. <https://doi.org/10.1088/1748-9326/aba867>
- Cobb, A. R., Hoyt, A. M., Gandois, L., Eri, J., Dommain, R., Abu Salim, K., et al. (2017). How temporal patterns in rainfall determine the geomorphology and carbon fluxes of tropical peatlands. *Proceedings of the National Academy of Sciences of the United States of America*, 114(26), E5187–E5196. <https://doi.org/10.1073/pnas.1701090114>
- Couwenberg, J., Dommain, R., & Joosten, H. (2010). Greenhouse gas fluxes from tropical peatlands in south-east Asia. *Global Change Biology*, 16(6), 1715–1732. <https://doi.org/10.1111/j.1365-2486.2009.02016.x>
- Couwenberg, J., & Hooijer, A. (2013). Toward robust subsidence-based soil carbon emission factors for peat soils in south-east Asia, with special reference to oil palm plantations. *Mires & Peat*, 12(1), 1–13.
- Cris, R., Buckmaster, S., Bain, C., & Reed, M. (2014). *Global peatland restoration demonstrating SUCCESS*. Edinburgh: IUCN UK National Committee Peatland Programme.
- Dadap, N. C., Cobb, A. R., Hoyt, A. M., Harvey, C. F., & Konings, A. G. (2019). Satellite soil moisture observations predict burned area in Southeast Asian peatlands. *Environmental Research Letters*, 14(9), 094014. <https://doi.org/10.1088/1748-9326/ab3891>
- Dargie, G. C., Lawson, I. T., Rayden, T. J., Miles, L., Mitchard, E. T. A., Page, S. E., et al. (2019). Congo Basin peatlands: Threats and conservation priorities. *Mitigation and Adaptation Strategies for Global Change*, 24(4), 669–686. <https://doi.org/10.1007/s11027-017-9774-8>
- Dargie, G. C., Lewis, S. L., Lawson, I. T., Mitchard, E. T. A., Page, S. E., Bocko, Y. E., & Ifo, S. A. (2017). Age, extent and carbon storage of the central Congo Basin peatland complex. *Nature*, 542(7639), 86–90. <https://doi.org/10.1038/nature21048>
- Dohong, A., Aziz, A. A., & Dargusch, P. (2017). A review of the drivers of tropical peatland degradation in South-East Asia. *Land Use Policy*, 69, 349–360. <https://doi.org/10.1016/j.landusepol.2017.09.035>
- Dommain, R., Couwenberg, J., & Joosten, H. (2010). Hydrological self-regulation of domed peatlands in south-east Asia and consequences for conservation and restoration. *Mires & Peat*, 6, 1–17.
- Evans, C. D., Williamson, J. M., Kacaribu, F., Irawan, D., Suardiwerianto, Y., Hidayat, M. F., et al. (2019). Rates and spatial variability of peat subsidence in Acacia plantation and forest landscapes in Sumatra, Indonesia. *Geoderma*, 338, 410–421. <https://doi.org/10.1016/j.geoderma.2018.12.028>
- Field, R. D., Van Der Werf, G. R., & Shen, S. S. P. P. (2009). Human amplification of drought-induced biomass burning in Indonesia since 1960. *Nature Geoscience*, 2(3), 185–188. <https://doi.org/10.1038/ngeo443>
- Gandois, L., Hoyt, A. M., Mounier, S., Le Roux, G., Harvey, C. F., Claustres, A., et al. (2020). From canals to the coast: Dissolved organic matter and trace metal composition in rivers draining degraded tropical peatlands in Indonesia. *Biogeosciences*, 17(7), 1897–1909. <https://doi.org/10.5194/bg-2019-253>
- Gorelick, N., Hancher, M., Dixon, M., Ilyushchenko, S., Thau, D., & Moore, R. (2017). Google Earth Engine: Planetary-scale geospatial analysis for everyone. *Remote Sensing of Environment*, 202, 18–27. <https://doi.org/10.1016/j.rse.2017.06.031>
- Günther, A., Barthelmes, A., Huth, V., Joosten, H., Jurasinski, G., Koesch, F., & Couwenberg, J. (2020). Prompt rewetting of drained peatlands reduces climate warming despite methane emissions. *Nature Communications*, 11(1), 1644. <https://doi.org/10.1038/s41467-020-15499-z>
- Hemes, K. S., Chamberlain, S. D., Eichelmann, E., Knox, S. H., & Baldocchi, D. D. (2018). A biogeochemical compromise: The high methane cost of sequestering carbon in restored wetlands. *Geophysical Research Letters*, 45(12), 6081–6091. <https://doi.org/10.1029/2018GL077747>
- Hiraishi, T., Krug, T., Tanabe, K., Srivastava, N., Baasansuren, J., Fukuda, M., & Troxler, T. G. (2014). *2013 Supplement to the 2006 IPCC Guidelines for National Greenhouse Gas Inventories: Wetlands Task Force on National Greenhouse Gas Inventories*. Switzerland.
- Hirano, T., Jauhainen, J., Inoue, T., & Takahashi, H. (2009). Controls on the carbon balance of tropical peatlands. *Ecosystems*, 12(6), 873–887. <https://doi.org/10.1007/s10021-008-9209-1>
- Hirano, T., Kusin, K., Limin, S., & Osaki, M. (2015). Evapotranspiration of tropical peat swamp forests. *Global Change Biology*, 21(5), 1914–1927. <https://doi.org/10.1111/gcb.12653>

- Hooijer, A., Page, S., Canadell, J. G., Silvius, M., Kwadijk, J., Wösten, H., & Jauhiainen, J. (2010). Current and future CO<sub>2</sub> emissions from drained peatlands in Southeast Asia. *Biogeosciences*, 7(5), 1505–1514. <https://doi.org/10.5194/bg-7-1505-2010>
- Hooijer, A., Page, S., Jauhiainen, J., Lee, W. A., Lu, X. X., Idris, A., & Anshari, G. (2012). Subsidence and carbon loss in drained tropical peatlands. *Biogeosciences*, 9(3), 1053–1071. <https://doi.org/10.5194/bg-9-1053-2012>
- Houterman, J., & Ritzema, H. P. (2009). *Land and water management in the Ex-Mega Rice Project area in central Kalimantan*. Technical Report No. 4, Master Plan for the Rehabilitation and Revitalisation of the Ex-Mega Rice Project Area, Central Kalimantan, Indonesia.
- Hoyt, A. M., Chaussard, E., Seppäläinen, S., & Harvey, C. (2020). Widespread subsidence and carbon emissions across Southeast Asia peatlands. *Nature Geoscience*, 13, 435–440. <https://doi.org/10.1038/s41561-020-0575-4>
- Hoyt, A. M., Gandois, L., Eri, J., Kai, F. M., Harvey, C. F., & Cobb, A. R. (2019). CO<sub>2</sub> emissions from an undrained tropical peatland: Interacting influences of temperature, shading and water table depth. *Global Change Biology*, 25(9), 2885–2899. <https://doi.org/10.1111/gcb.14702>
- Jaenicke, J., Wösten, H., Budiman, A., & Siegert, F. (2010). Planning hydrological restoration of peatlands in Indonesia to mitigate carbon dioxide emissions. *Mitigation and Adaptation Strategies for Global Change*, 15(3), 223–239. <https://doi.org/10.1007/s11027-010-9214-5>
- Jauhiainen, J., Hooijer, A., & Page, S. E. (2012). Carbon dioxide emissions from an Acacia plantation on peatland in Sumatra, Indonesia. *Biogeosciences*, 9(2), 617–630. <https://doi.org/10.5194/bg-9-617-2012>
- Jauhiainen, J., & Silvennoinen, H. (2012). Diffusion GHG fluxes at tropical peatland drainage canal water surfaces. *Suo*, 63(3–4), 93–105.
- Jauhiainen, J., Takahashi, H., Heikkinen, J. E. P., Martikainen, P. J., & Vasander, H. (2005). Carbon fluxes from a tropical peat swamp forest floor. *Global Change Biology*, 11(10), 1788–1797. <https://doi.org/10.1111/j.1365-2486.2005.001031.x>
- Konecny, K., Ballhorn, U., Navratil, P., Jubanski, J., Page, S. E., Tansey, K., et al. (2016). Variable carbon losses from recurrent fires in drained tropical peatlands. *Global Change Biology*, 22(4), 1469–1480. <https://doi.org/10.1111/gcb.13186>
- Kopitz, S. N., Mickley, L. J., Marlier, M. E., Buonocore, J. J., Kim, P. S., Liu, T., et al. (2016). Public health impacts of the severe haze in Equatorial Asia in September–October 2015: Demonstration of a new framework for informing fire management strategies to reduce downwind smoke exposure. *Environmental Research Letters*, 11(9), 094023. <https://doi.org/10.1088/1748-9326/11/9/094023>
- Krizhevsky, A., Sutskever, I., & Hinton, G. E. (2017). ImageNet classification with deep convolutional neural networks. *Communications of the ACM*, 60(6), 84–90. <https://doi.org/10.1145/3065386>
- Kurnianto, S., Selker, J., Boone Kauffman, J., Murdiyarso, D., & Peterson, J. T. (2018). *The influence of land-cover changes on the variability of saturated hydraulic conductivity in tropical peatlands*. In *Mitigation and adaptation strategies for global change* (pp. 1–21). <https://doi.org/10.1007/s11027-018-9802-3>
- LeCun, Y., Bottou, L., Bengio, Y., & Haffner, P. (1998). Gradient-based learning applied to document recognition. *Proceedings of the IEEE*, 86(11), 2278–2323. <https://doi.org/10.1109/5.726791>
- Leifeld, J., & Menichetti, L. (2018). The underappreciated potential of peatlands in global climate change mitigation strategies. *Nature Communications*, 9(1), 1071. <https://doi.org/10.1038/s41467-018-03406-6>
- Leifeld, J., Müller, M., & Fuhrer, J. (2011). Peatland subsidence and carbon loss from drained temperate fens. *Soil Use & Management*, 27(2), 170–176. <https://doi.org/10.1111/j.1475-2743.2011.00327.x>
- Leifeld, J., Wüst-Galley, C., & Page, S. (2019). Intact and managed peatland soils as a source and sink of GHGs from 1850 to 2100. *Nature Climate Change*, 9(12), 945–947. <https://doi.org/10.1038/s41558-019-0615-5>
- Lilleskov, E., McCullough, K., Hergoualc'h, K., del Castillo Torres, D., Chimner, R., Murdiyarso, D., et al. (2019). Is Indonesian peatland loss a cautionary tale for Peru? A two-country comparison of the magnitude and causes of tropical peatland degradation. *Mitigation and Adaptation Strategies for Global Change*, 24(4), 591–623. <https://doi.org/10.1007/s11027-018-9790-3>
- Lim, K. H., Lim, S. S., Parish, F., & Suharto, R. (2012). *RSPO manual on best management practices (BMPs) for existing oil palm cultivation on peat*. Kuala Lumpur, Malaysia: RSPO.
- Manoli, G., Meijide, A., Huth, N., Knohl, A., Kosugi, Y., Burlando, P., et al. (2018). Ecohydrological changes after tropical forest conversion to oil palm. *Environmental Research Letters*, 13(6), 064035. <https://doi.org/10.1088/1748-9326/aac54e>
- Mezbahuddin, M., Grant, R. F., & Hirano, T. (2015). How hydrology determines seasonal and interannual variations in water table depth, surface energy exchange, and water stress in a tropical peatland: Modeling versus measurements. *Journal of Geophysical Research: Biogeosciences*, 120(11), 2132–2157. <https://doi.org/10.1002/2015JG003005>
- Miettinen, J., Hooijer, A., Vernimmen, R., Liew, S. C., & Page, S. E. (2017). From carbon sink to carbon source: Extensive peat oxidation in insular Southeast Asia since 1990. *Environmental Research Letters*, 12(2), 024014. <https://doi.org/10.1088/1748-9326/aa5b6f>
- Miettinen, J., Hooijer, A., Wang, J., Shi, C., & Liew, S. C. (2012). Peatland degradation and conversion sequences and interrelations in Sumatra. *Regional Environmental Change*, 12(4), 729–737. <https://doi.org/10.1007/s10113-012-0290-9>
- Miettinen, J., Shi, C., & Liew, S. C. (2016). Land cover distribution in the peatlands of Peninsular Malaysia, Sumatra and Borneo in 2015 with changes since 1990. *Global Ecology and Conservation*, 6, 67–78. <https://doi.org/10.1016/j.gecco.2016.02.004>
- Moore, S., Evans, C. D., Page, S. E., Garnett, M. H., Jones, T. G., Freeman, C., et al. (2013). Deep instability of deforested tropical peatlands revealed by fluvial organic carbon fluxes. *Nature*, 493(7434), 660–663. <https://doi.org/10.1038/nature11818>
- Morecroft, M. D., Duffield, S., Harley, M., Pearce-Higgins, J. W., Stevens, N., Watts, O., & Whitaker, J. (2019). Measuring the success of climate change adaptation and mitigation in terrestrial ecosystems. *Science*, 366(6471), eaaw9256. <https://doi.org/10.1126/science.aaw9256>
- Murdiyarso, D., Hergoualc'h, K., Verchot, L. V., Pittman, A. M., Soares-Filho, B. S., Asner, G. P., et al. (2010). Opportunities for reducing greenhouse gas emissions in tropical peatlands. *Proceedings of the National Academy of Sciences of the United States of America*, 107(46), 19655–19660. <https://doi.org/10.1073/pnas.0911966107>
- Oner, D., Kozinski, M., Citraro, L., Dadap, N. C., Konings, A. G., & Fua, P. (2020). *Promoting connectivity of network-like structures by enforcing region separation*. ArXiv. Retrieved from <http://arxiv.org/abs/2009.07011>
- Page, S. E., Rieley, J. O., & Banks, C. J. (2011). Global and regional importance of the tropical peatland carbon pool. *Global Change Biology*, 17(2), 798–818. <https://doi.org/10.1111/j.1365-2486.2010.02279.x>
- Page, S. E., Siegert, F., Rieley, J. O., Boehm, H.-D. V., Jaya, A., & Limin, S. (2002). The amount of carbon released from peat and forest fires in Indonesia during 1997. *Nature*, 420(6911), 61–65. <https://doi.org/10.1038/nature01131>
- Planet Team. (2017). *Planet application program interface*. In *Space for life on Earth*. San Francisco, CA.
- Rahman, M. M., McDermid, G. J., Strack, M., & Lovitt, J. (2017). A new method to map groundwater table in peatlands using unmanned aerial vehicles. *Remote Sensing*, 9(10), 1057. <https://doi.org/10.3390/rs9101057>
- Republic of Indonesia. (2016). *Government Regulation of the Republic of Indonesia No. 57 of 2016, Amendment to Government Regulation No. 71 of 2014 on the Protection and management of Peat Ecosystems*. Retrieved from <http://peraturan.go.id/pp/nomor-57-tahun-2016.html>

- Roelens, J., Höfle, B., Dondeyne, S., Van Orshoven, J., & Diels, J. (2018). Drainage ditch extraction from airborne LiDAR point clouds. *ISPRS Journal of Photogrammetry and Remote Sensing*, *146*(May), 409–420. <https://doi.org/10.1016/j.isprsjprs.2018.10.014>
- Ronneberger, O., Fischer, P., & Brox, T. (2015). *U-net: Convolutional networks for biomedical image segmentation*. Lecture Notes in Computer Science (including subseries Lecture Notes in Artificial Intelligence and Lecture Notes in Bioinformatics) (Vol. 9351, pp. 234–241). Springer Verlag. [https://doi.org/10.1007/978-3-319-24574-4\\_28](https://doi.org/10.1007/978-3-319-24574-4_28)
- Schroeder, W., Oliva, P., Giglio, L., & Csiszar, I. A. (2014). The New VIIRS 375 m active fire detection data product: Algorithm description and initial assessment. *Remote Sensing of Environment*, *143*, 85–96. <https://doi.org/10.1016/j.rse.2013.12.008>
- Simpson, J. E., Wooster, M. J., Smith, T. E. L., Trivedi, M., Vernimmen, R. R. E., Dedi, R., et al. (2016). Tropical peatland burn depth and combustion heterogeneity assessed using UAV photogrammetry and airborne LiDAR. *Remote Sensing*, *8*(12), 1000. <https://doi.org/10.3390/rs8121000>
- Sinclair, A. L., Graham, L. L. B., Putra, E. I., Saharjo, B. H., Applegate, G., Grover, S. P., & Cochrane, M. A. (2020). Effects of distance from canal and degradation history on peat bulk density in a degraded tropical peatland. *Science of the Total Environment*, *699*, 134199. <https://doi.org/10.1016/j.scitotenv.2019.134199>
- Sloan, S., Locatelli, B., Wooster, M. J., & Gaveau, D. L. A. (2017). Fire activity in Borneo driven by industrial land conversion and drought during El Niño periods, 1982–2010. *Global Environmental Change*, *47*, 95–109. <https://doi.org/10.1016/j.gloenvcha.2017.10.001>
- Suryadiputra, N., Dohong, A., Waspodo, R., Lubis, I., Hasudungan, F., & Wibisono, I. T. (2005). *A guide to blocking of canals and ditches in conjunction with the community*. In Wetlands International–Indonesia Programme. Bogor.
- Sze, J. S., & Lee, J. S. H. (2018). Evaluating the social and environmental factors behind the 2015 extreme fire event in Sumatra, Indonesia. *Environmental Research Letters*, *14*, 015001. <https://doi.org/10.1088/1748-9326/aee1d>
- Tanneberger, F., Appulo, L., Ewert, S., Lakner, S., Ó Brolcháin, N., Peters, J., & Wichtmann, W. (2020). The power of nature-based solutions: How peatlands can help us to achieve key EU sustainability objectives. *Advanced Sustainable Systems*, *5*, 2000146. <https://doi.org/10.1002/adsu.202000146>
- Taufik, M., Minasny, B., McBratney, A. B., Van Dam, J., Jones, P., & Van Lanen, H. (2020). Human-induced changes in Indonesia peatlands increase drought severity. *Environmental Research Letters*, *15*, 084013.
- Tiemeyer, B., Freibauer, A., Borraz, E. A., Augustin, J., Bechtold, M., Beetz, S., et al. (2020). A new methodology for organic soils in national greenhouse gas inventories: Data synthesis, derivation and application. *Ecological Indicators*, *109*, 105838. <https://doi.org/10.1016/j.ecolind.2019.105838>
- Usup, A., Hashimoto, Y., Takahashi, H., & Hayasaka, H. (2004). Combustion and thermal characteristics of peat fire in tropical peatland in Central Kalimantan, Indonesia. *Tropics*, *14*, 1–19.
- van den Akker, J., Kuikman, P., De Vries, F., Hoving, I., Pleijter, M., Hendriks, R., et al. (2008). *Emission of CO<sub>2</sub> from agricultural peat soils in the Netherlands and ways to limit this emission*. Proceedings of the 13th International Peat Congress after wise use – The future of peatlands, Vol. 1 Oral presentations, Tullamore, Ireland (pp. 645–648). Jyväskylä, Finland. Retrieved from <https://library.wur.nl/WebQuery/wurpubs/fulltext/159747>
- Van den Wyngaert, I. (2008). *Greenhouse gas reporting of the LULUCF sector, revisions and updates related to the Dutch NIR 2008*. Staff Publications.
- van der Werf, G. R., Dempewolf, J., Trigg, S. N., Randerson, J. T., Kasibhatla, P. S., Giglio, L., et al. (2008). Climate regulation of fire emissions and deforestation in equatorial Asia. *Proceedings of the National Academy of Sciences of the United States of America*, *105*(51), 20350–20355. <https://doi.org/10.1073/pnas.0803375105>
- van Lent, J., Hergoualc'h, K., Verchot, L., Oenema, O., & van Groenigen, J. W. (2019). Greenhouse gas emissions along a peat swamp forest degradation gradient in the Peruvian Amazon: Soil moisture and palm roots effects. *Mitigation and Adaptation Strategies for Global Change*, *24*(4), 625–643. <https://doi.org/10.1007/s11027-018-9796-x>
- Vernimmen, R., Hooijer, A., Akmalia, R., Fitriatanegara, N., Mulyadi, D., Yuherdha, A., et al. (2020a). Mapping deep peat carbon stock from a LiDAR based DTM and field measurements, with application to eastern Sumatra. *Carbon Balance and Management*, *15*(1), 4. <https://doi.org/10.1186/s13021-020-00139-2>
- Vernimmen, R., Hooijer, A., Mulyadi, D., Setiawan, I., Pronk, M., & Yuherdha, A. T. (2020b). A new method for rapid measurement of canal water table depth using airborne LiDAR, with application to drained peatlands in Indonesia. *Water (Switzerland)*, *12*(5), 1486. <https://doi.org/10.3390/w12051486>
- Vetrita, Y., & Cochrane, M. A. (2020). Fire frequency and related land-use and land-cover changes in Indonesia's peatlands. *Remote Sensing*, *12*(1), 5. <https://doi.org/10.3390/RS12010005>
- Warren, M., Hergoualc'h, K., Kauffman, J. B., Murdiyarto, D., & Kolka, R. (2017). An appraisal of Indonesia's immense peat carbon stock using national peatland maps: Uncertainties and potential losses from conversion. *Carbon Balance and Management*, *12*, 12. <https://doi.org/10.1186/s13021-017-0080-2>
- Wedeux, B., Dalponte, M., Schlund, M., Hagen, S., Cochrane, M., Graham, L., et al. (2020). *Dynamics of a human-modified tropical peat swamp forest revealed by repeat lidar surveys*. In Global Change Biology. <https://doi.org/10.1111/gcb.15108>
- Wells, J. A., Wilson, K. A., Abram, N. K., Nunn, M., Gaveau, D. L. A., Runting, R. K., et al. (2016). Rising floodwaters: Mapping impacts and perceptions of flooding in Indonesian Borneo. *Environmental Research Letters*, *11*, 064016. <https://doi.org/10.1088/1748-9326/11/6/064016>
- Wiedemann, C., Heipke, C., Mayer, H., & Jamet, O. (1998). *Empirical evaluation of automatically extracted road axes*. In Empirical evaluation techniques in computer vision (pp. 172–187).
- Wilson, D., Blain, D., Couwenberg, J., Evans, C. D., Murdiyarto, D., Page, S. E., et al. (2016). Greenhouse gas emission factors associated with rewetting of organic soils. *Mires & Peat*, *17*(04), 1–28. <https://doi.org/10.19189/Map.2016.OMB.222>